29.11.99

RESULTS OF THE ELECTRON GUN BEAM DYNAMICS SIMULATIONS AND MEASUREMENTS.

Head of the work: Avraham Gover
Simulations: Sergey Efimov
Experiment: Vladimir Batenkov, Jerzy Sokolowski and Michael Canter
Editing and discussions: Arie Eichenbaum

Results of the EGUN code simulations and comparison with measured beam sizes on a screen for 60kV and 43kV cathode – anode voltages and for different currents of the two focusing coils (short solenoids) are reported herein.

1. For 60kV cathode-anode voltage.

Simulation parameters: beam current I_{beam}=**1.09A**;
grid – cathode voltage U_{grid}=13kV.

Electron trajectories from the electron gun cathode to the screen (located 741 mm from the cathode) are shown in the Fig.1. Two coils, the first C1 (of average radius 68.5 mm, 200 turns) and the second C2 (of average radius 135mm, 420 turns) as shown in Fig.1 are used. The simulated radial current density distribution and the respective beam phase- space on the screen are shown in the Figs.2 and Fig.3. 200 particles were used for simulations. On the screen plan we may note the halo around the beam due to space charge (see Figs 1, 2 and 3). For comparing beam dynamics results for a very low current are shown on the Fig.4 – Fig.5.

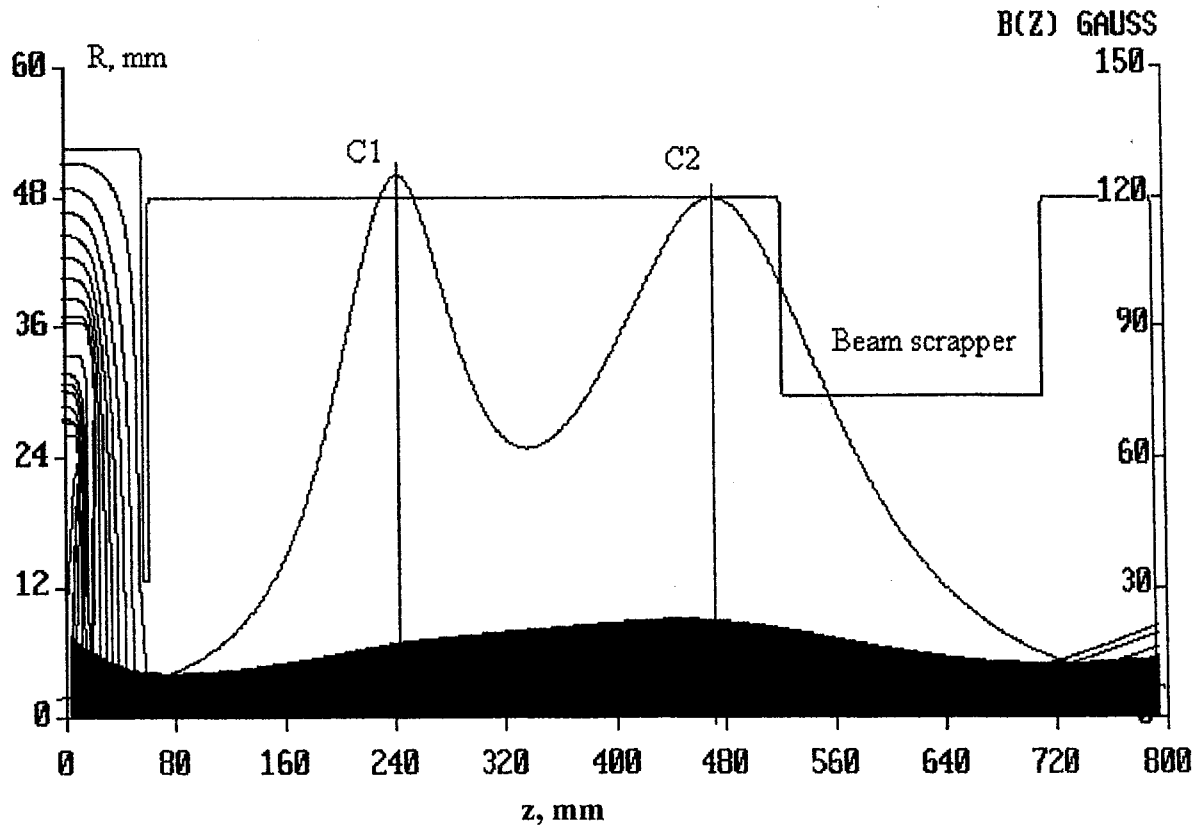

Fig.1. Electron trajectories for I_{beam}=**1.09A**. Coil currents are: I(coil 1)=I(coil 2)=**6A**.

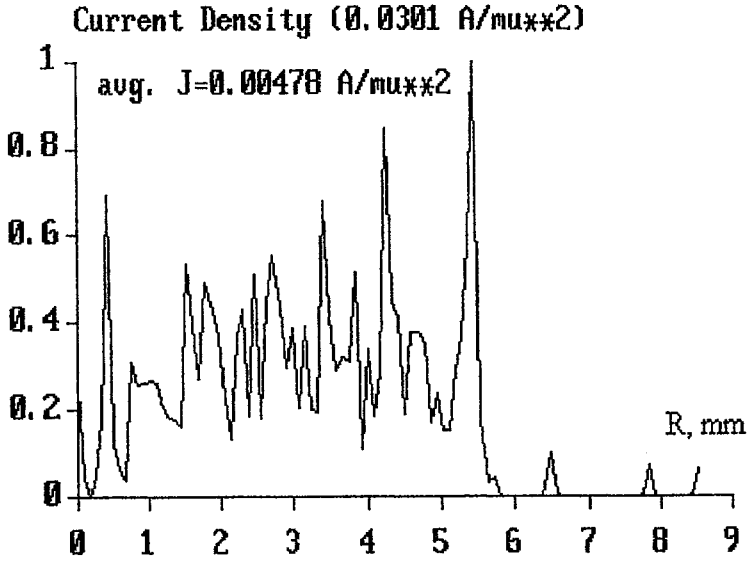

Fig.2. Radial beam density distribution in the screen for I_{beam}=**1.09A.**, I(coil 1)= I(coil 2) = **6**A .

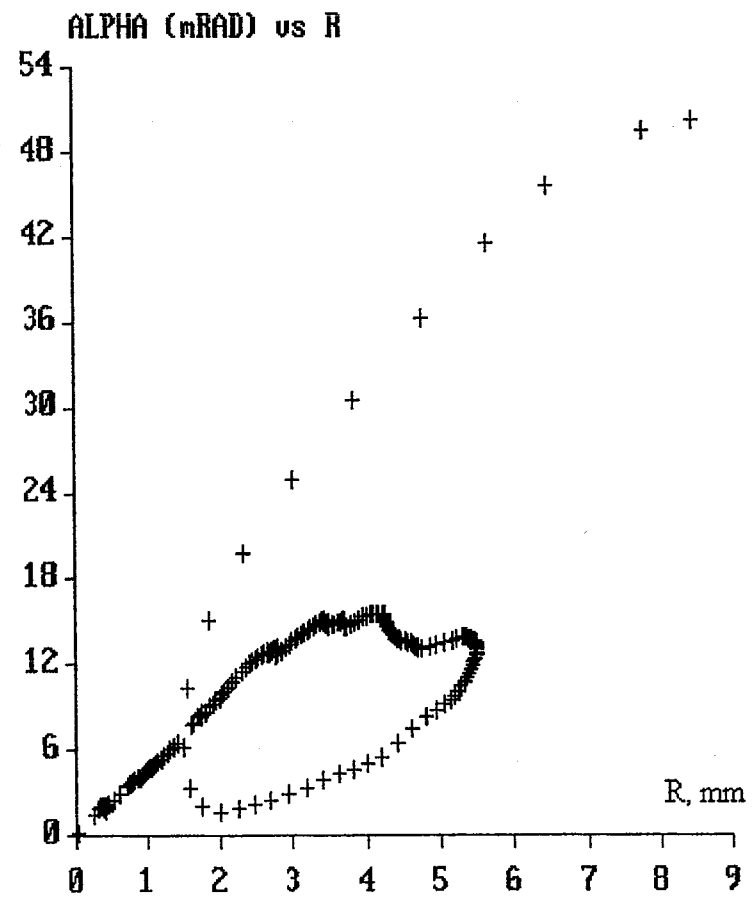

Fig.3. Electrons in the phase-space in the screen position for I_{beam}=**1.09A,** I(coil 1) =I(coil 2) = **6**A .

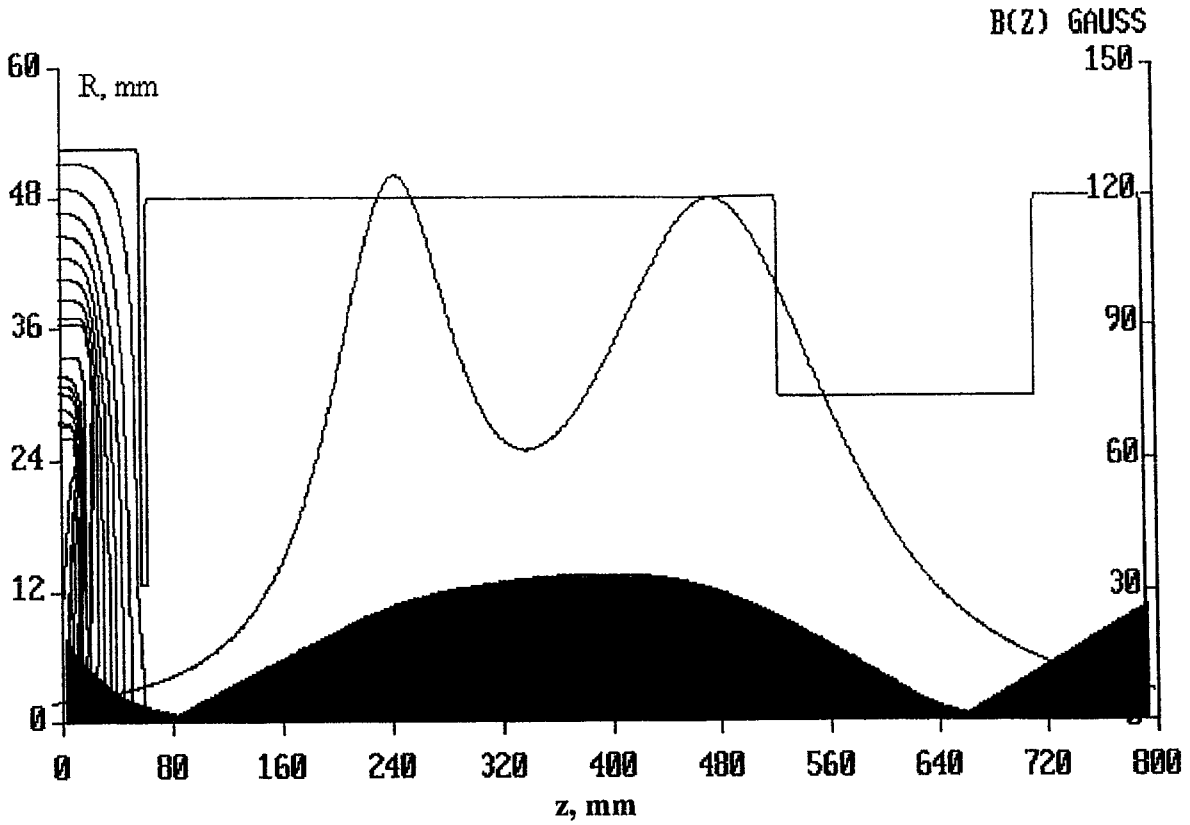

Fig.4. Electron trajectories for very low beam current (no space charge). Coil currents are: I(coil 1)=I(coil 2) = 6A.

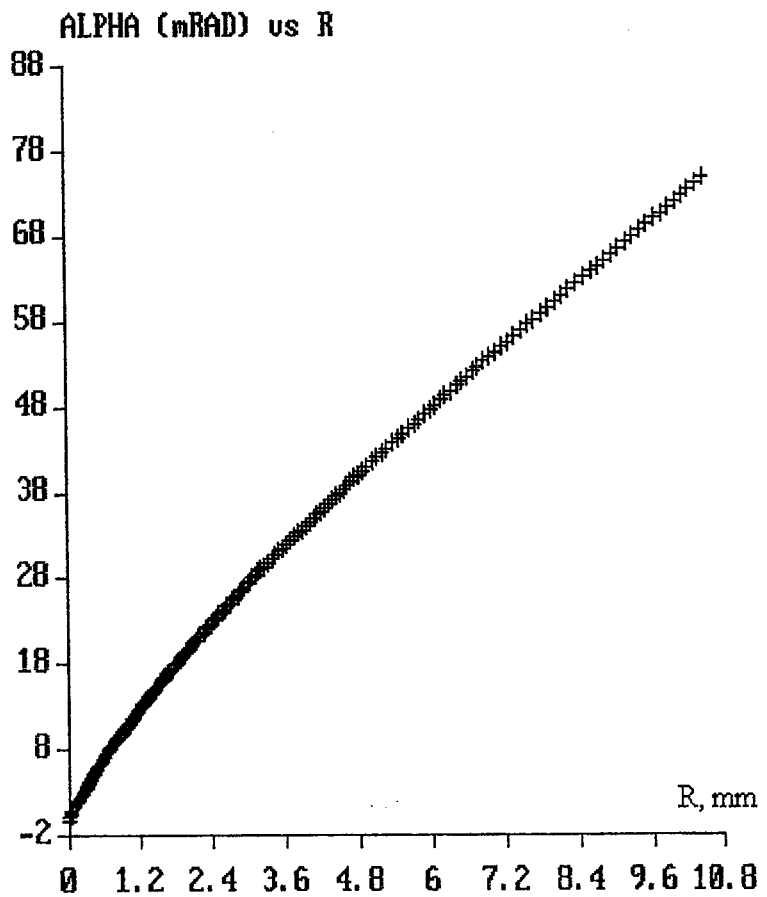

Fig.5. Electrons in the phase space on the screen for I_{beam}=0A, I(coil 1)=I(coil 2)= 6A.

For solenoids which are sufficiently far apart so that their fields do not overlap the current direction does not effect the focusing. In our case the distance between the two solenoids is not sufficiently large so that then is an overlap of magnetic fields and, therefore, reversing of current direction in the coils influence the focusing. Results of simulations for opposite directed coil currents and I_{beam} =1.09A are presented in the Figs. 6-8.

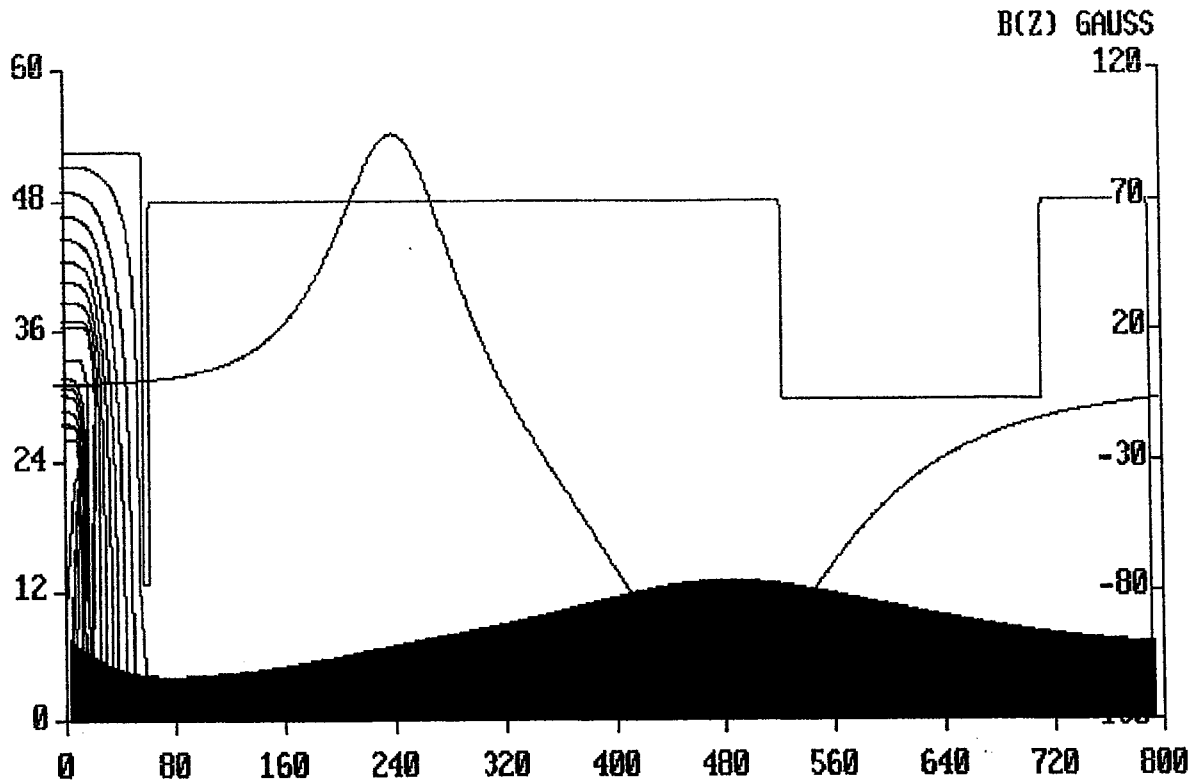

Fig.6. Electron trajectories for I_{beam}=**1.09A**. Coil currents are: I(coil 1) =**6A**, I(coil 2) = **-6A**.

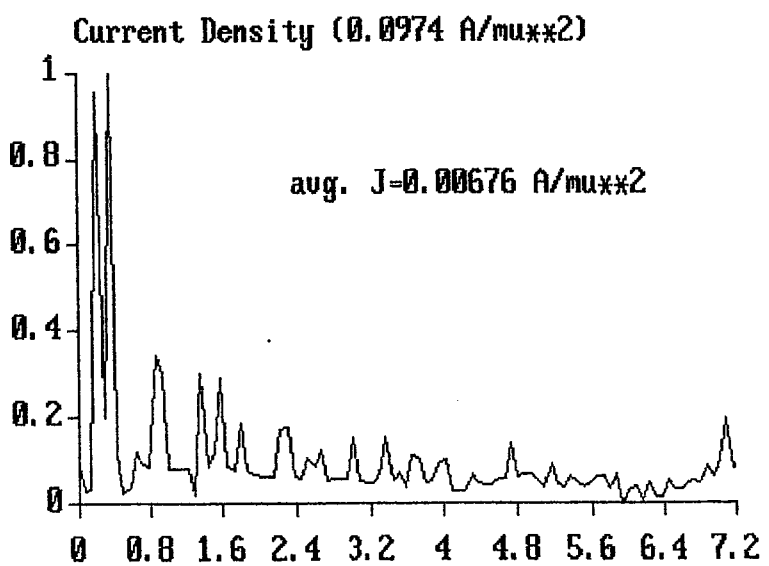

Fig.7. Radial beam density distribution on the screen for I_{beam}=**1.09A** and for **oppositely** directed currents of coils (**6**Amp for C1 and **–6**Amp for C2).

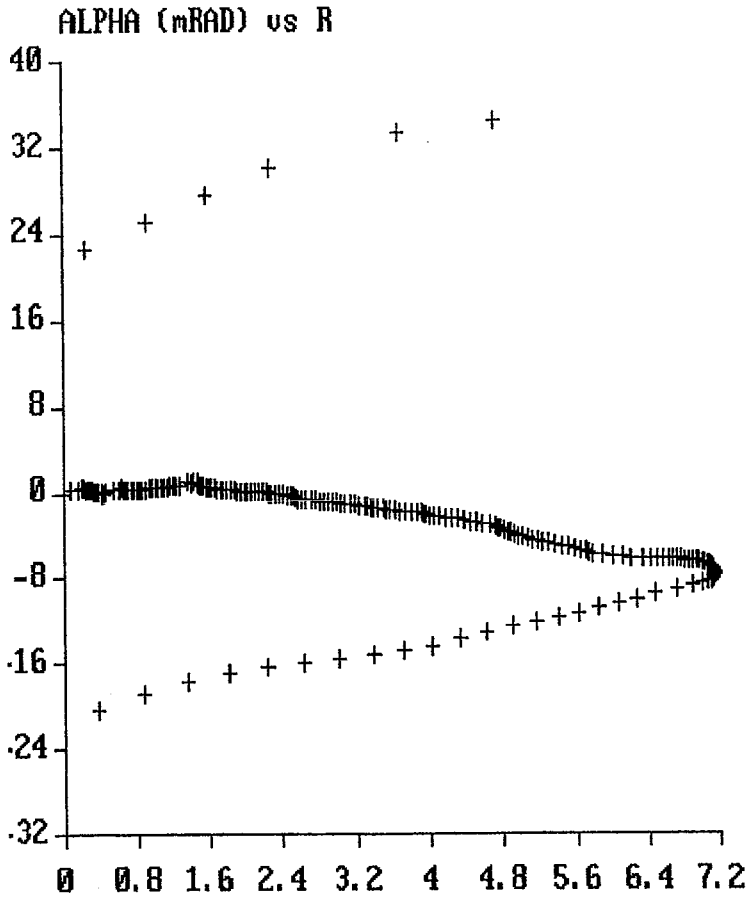

Fig.8. Electrons in phase space for I_{beam}=**1.09A** and for **oppositely** directed coil currents (**6**Amp and –**6**Amp)

Fig.9 – Fig.11 illustrate the electron tracing for one focusing coil (only the second coil is used). It is shown that the beam size on the screen is not larger than the size for the case of two focusing solenoids. The beam divergence and the effective emittance are larger for this case. The maximum beam envelope is larger also.

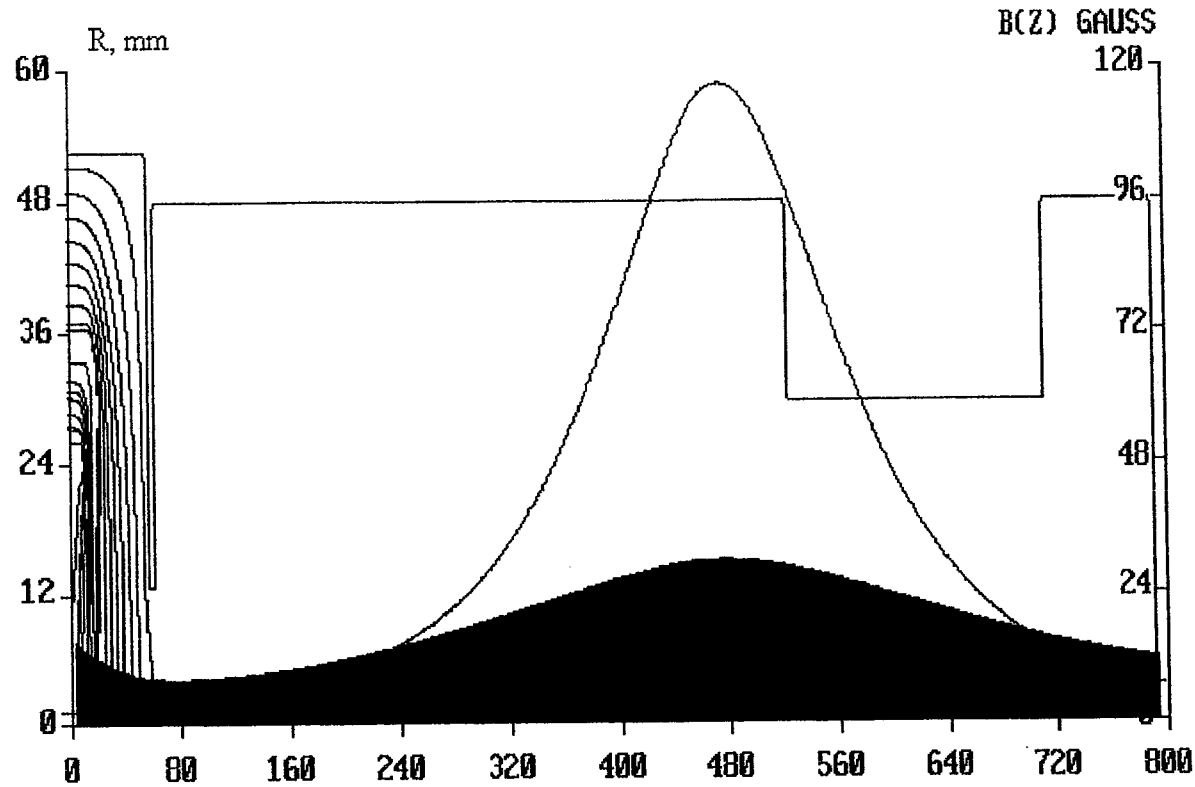

Fig.9. Electron trajectories for I_{beam}=**1.09A**. Coil currents are: I(coil 1) =**0A**, I(coil 2) = **6A**.

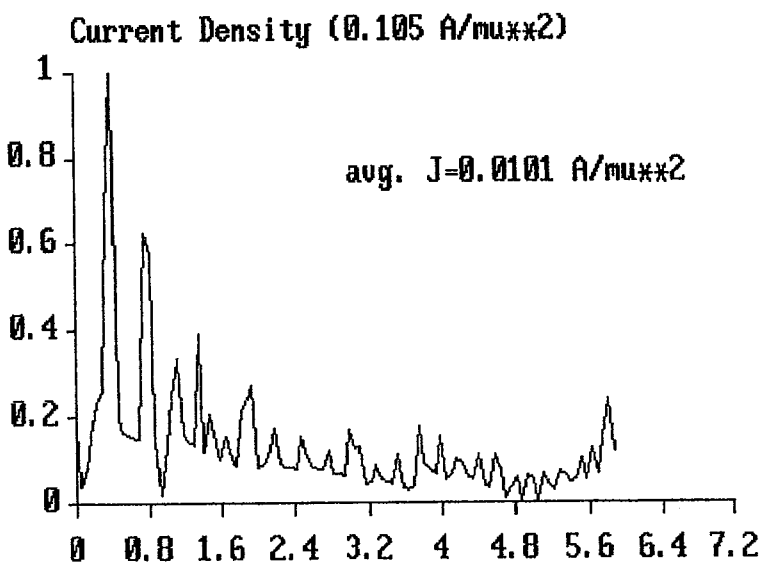

Fig.10. Radial beam density distribution on the screen for I_{beam}=**1.09A**, I(coil 1) =0, I(coil 2) = **6A** .

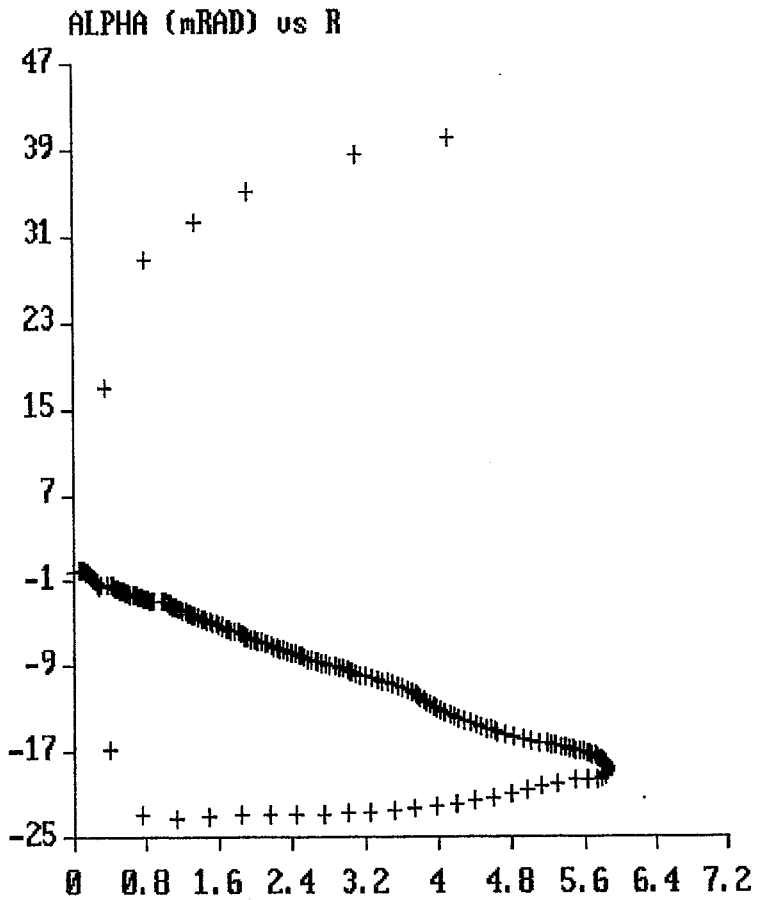

Fig.11. Electrons phase space at the screen position for I_{beam}=**1.09A**, I(coil 1) =**0**, I(coil 2) = **6**A .

The direction of the current in the coils which were used in the experiments was the same. Results of simulations and the beam diameters measured on the screen are shown in Figs12-19. These results were obtained using a constant coil1 current while the current in coil2 as a variable. At the bottom of the each figure part of the full picture is shown in the larger scale. Horizontal line on the level 30mm indicates a limit of the measured beam diameter.

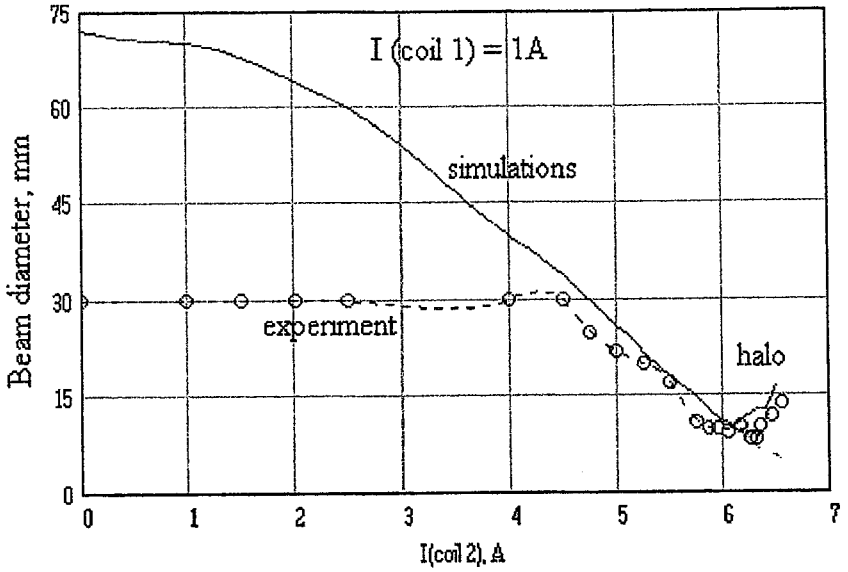

a).

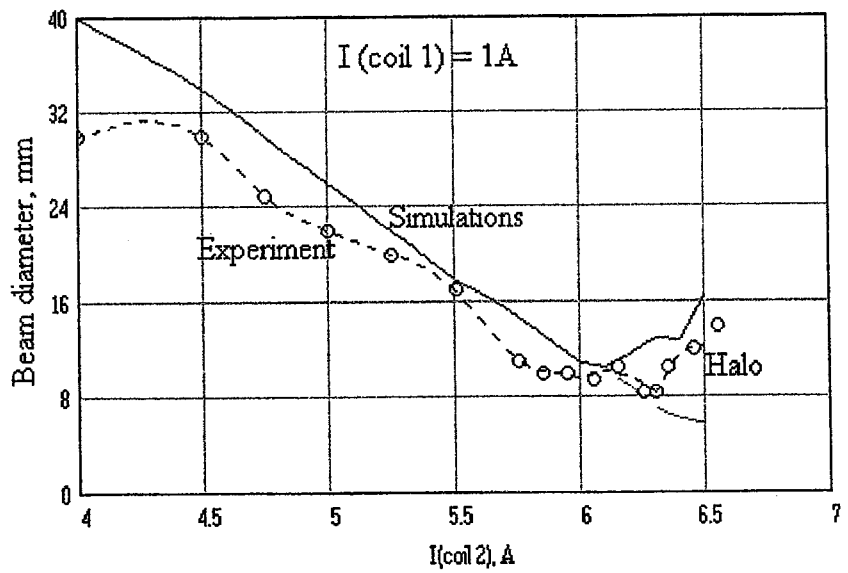

b).

Fig.12a. Simulated and experimental measured beam diameter at the screen position. I (coil1) = 1A and I (coil 2) varied.

Fig.12b. Expansion of the Fig.12a for coil 2 current above 4 Amp.

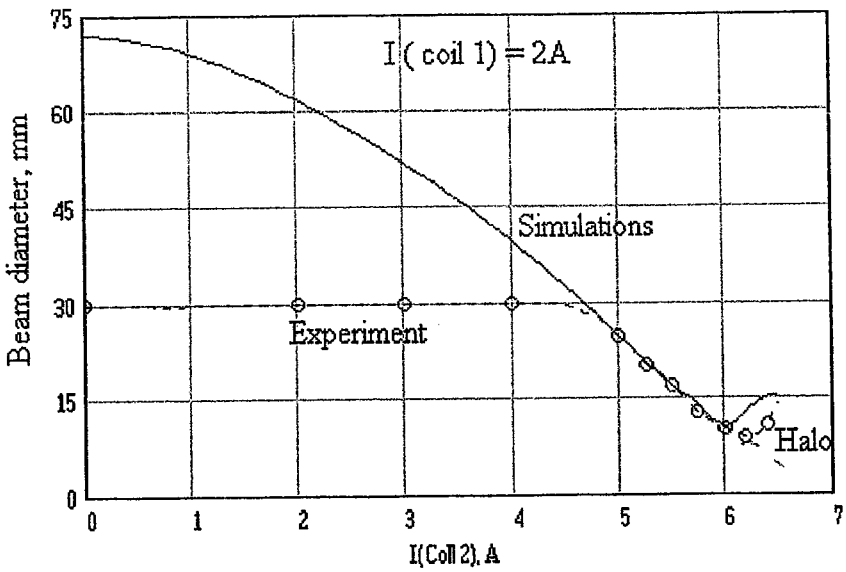

a).

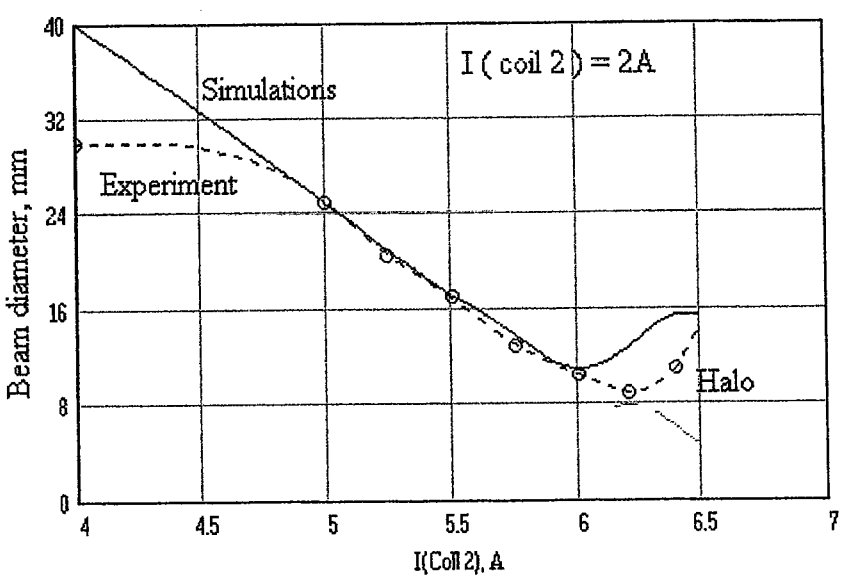

b).

Fig.13a. Simulated and experimental measured beam diameter at the screen position. I (coil1) = 2A and I (coil 2) varied.

Fig.13b. Expansion of the Fig.13a for coil 2 current above 4 Amps.

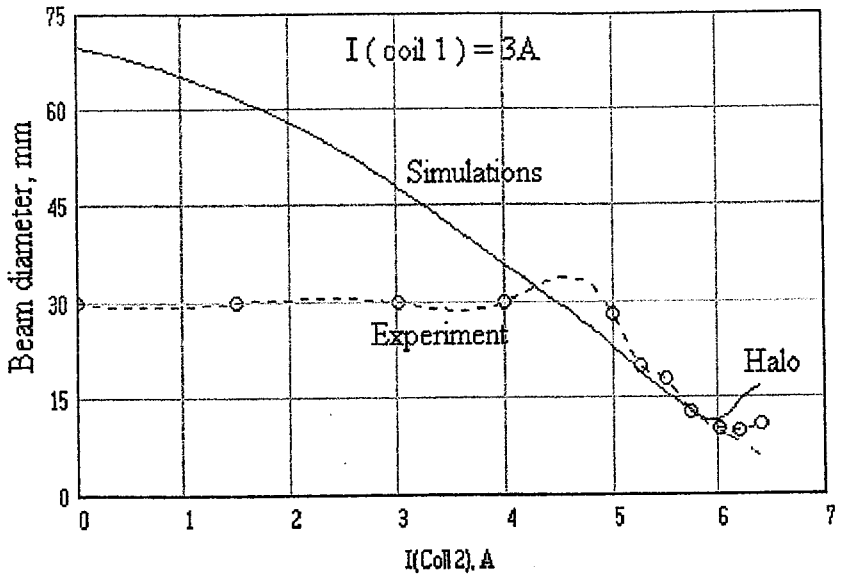

a).

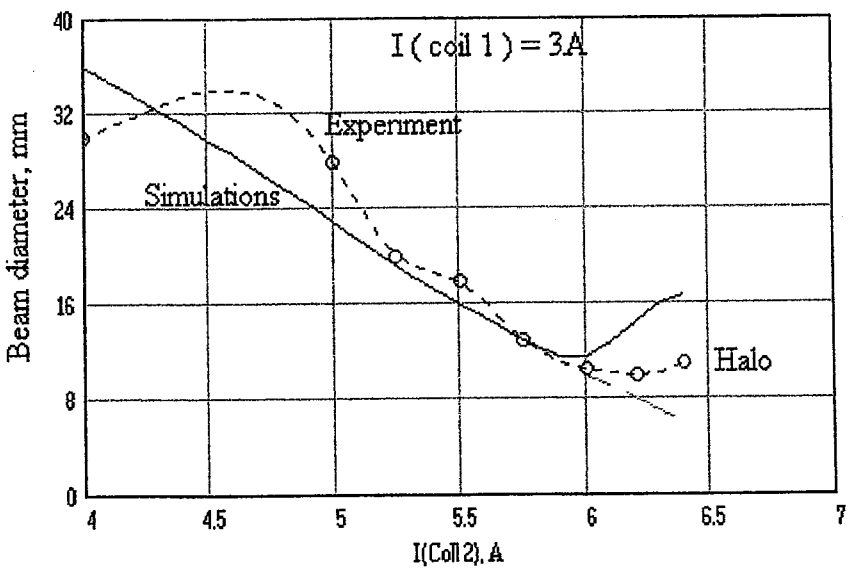

b).

Fig.14a. Simulated and experimental measured beam diameter at the screen position. I (coil1) = 3A and I (coil 2) varied.

Fig.14b. Expansion of the Fig.14a for coil 2 current above 4 Amps.

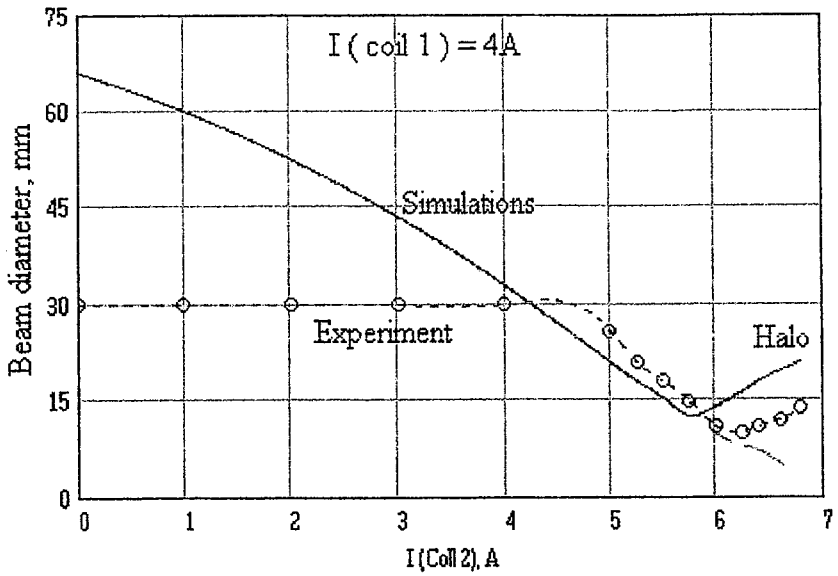

a).

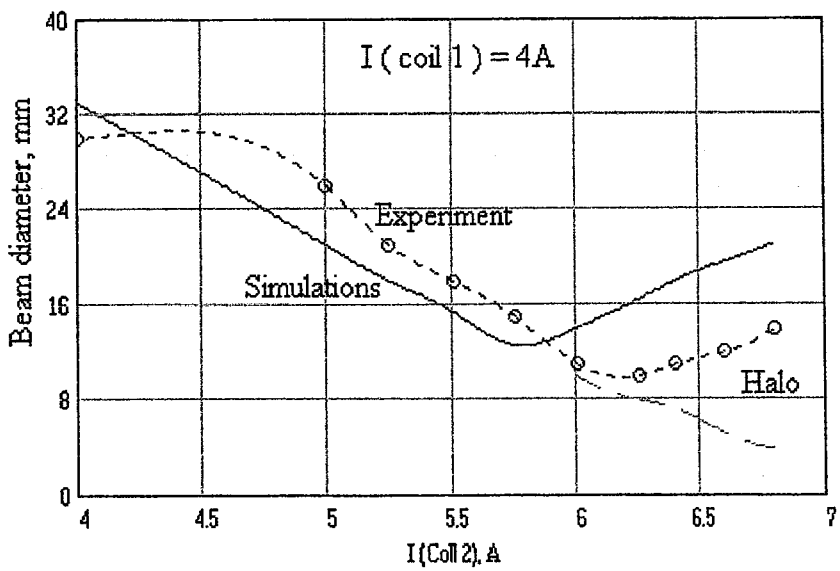

b).

Fig.15a. Simulated and experimental measured beam diameter at the screen position. I (coil1) = 4A and I (coil 2) varied.

Fig.15b. Expansion of the Fig.15a for coil 2 current above 4 Amps.

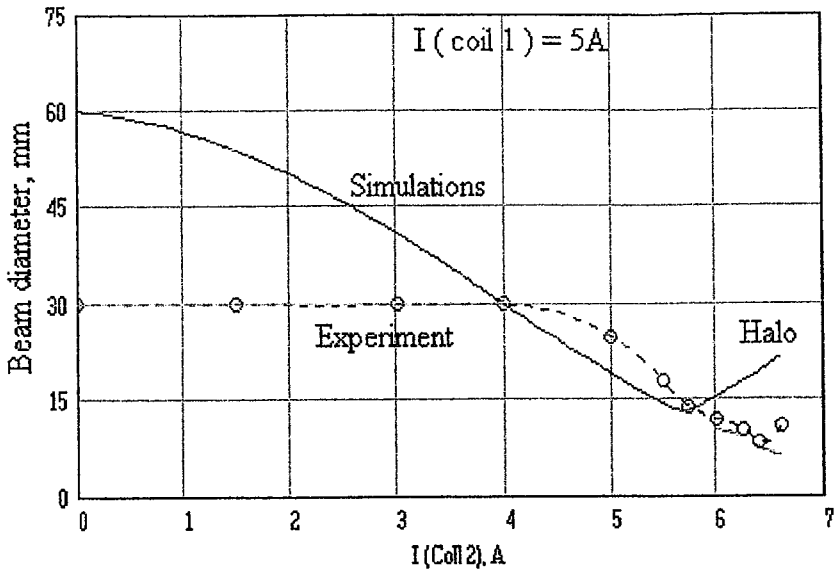

a).

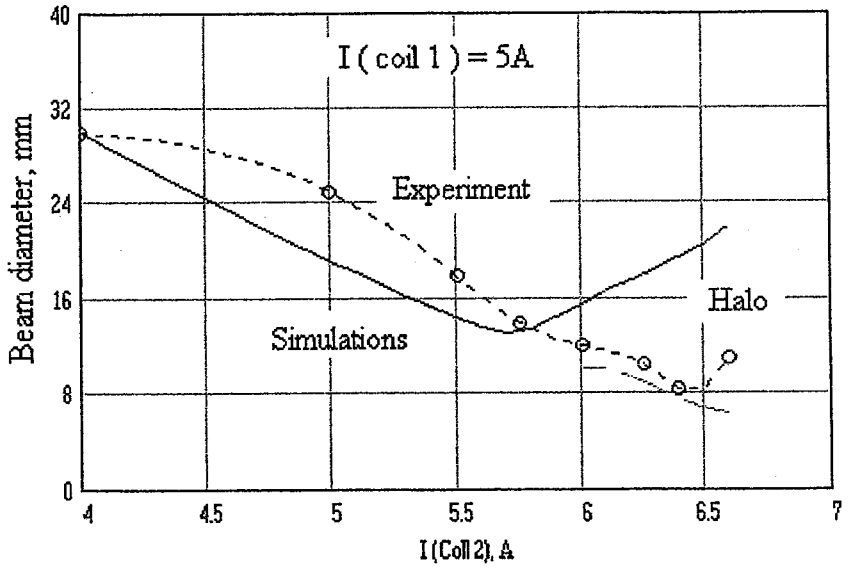

b).

Fig.16a. Simulated and experimental measured beam diameter at the screen position. I (coil1) = 5A and I (coil 2) varied.

Fig.16b. Expansion of the Fig.16a for coil 2 current above 4 Amps.

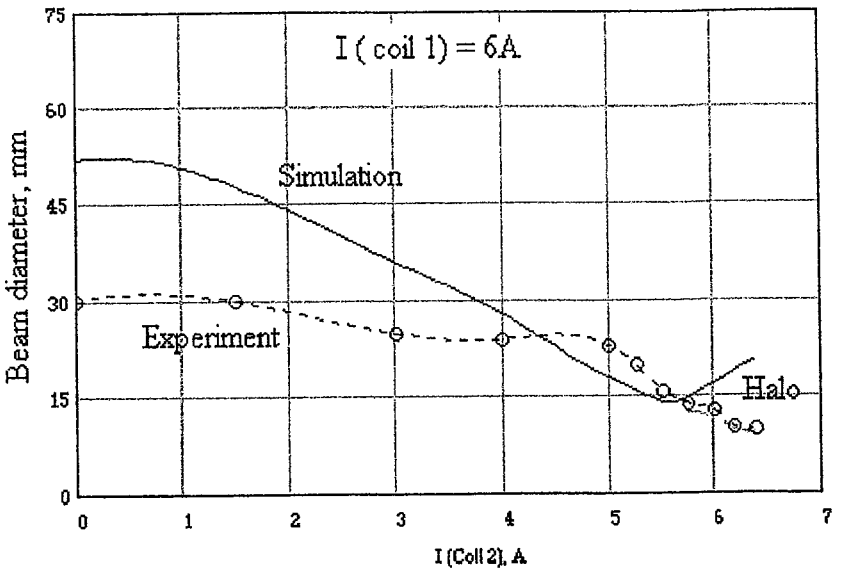

a).

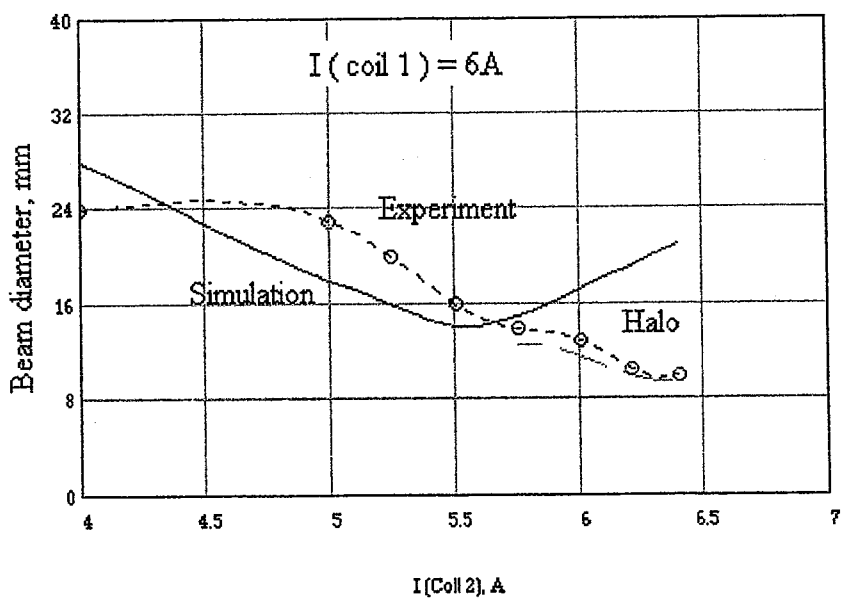

b).

Fig.17a. Simulated and experimental measured beam diameter at the screen position. I (coil1) = 6A and I (coil 2) varied.

Fig.17b. Expansion of the Fig.17a for coil 2 current above 4 Amps.

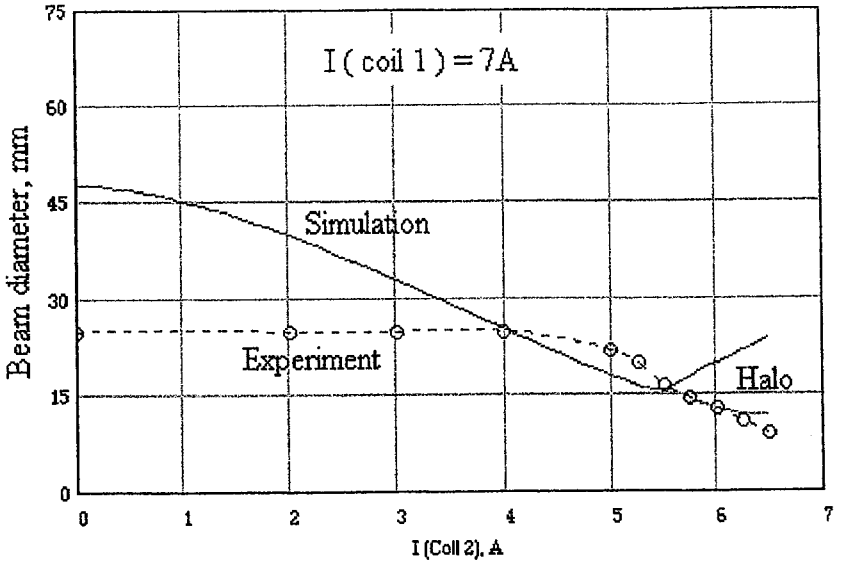

a).

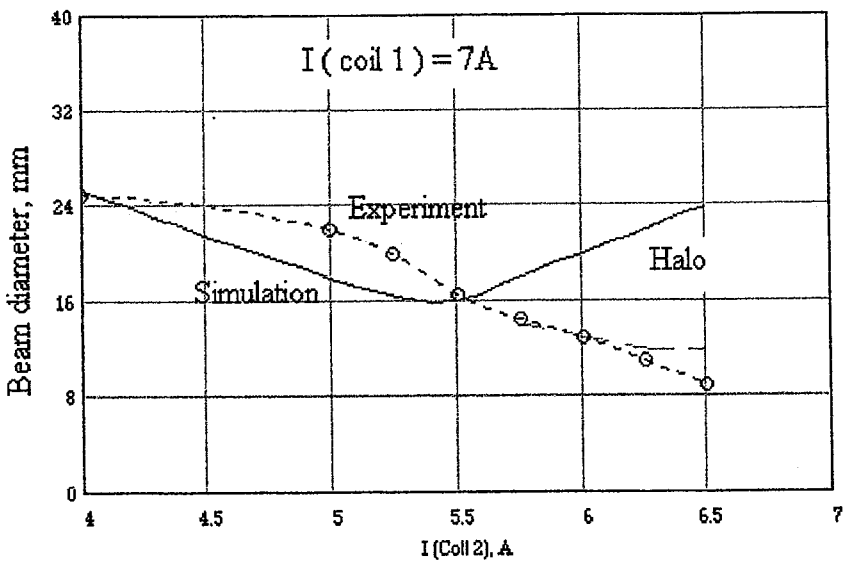

b).

Fig.18a. Simulated and experimental measured beam diameter at the screen position. I (coil1) = 7A and I (coil 2) varied.

Fig.18b. Expansion of the Fig.18a for coil 2 current above 4 Amps.

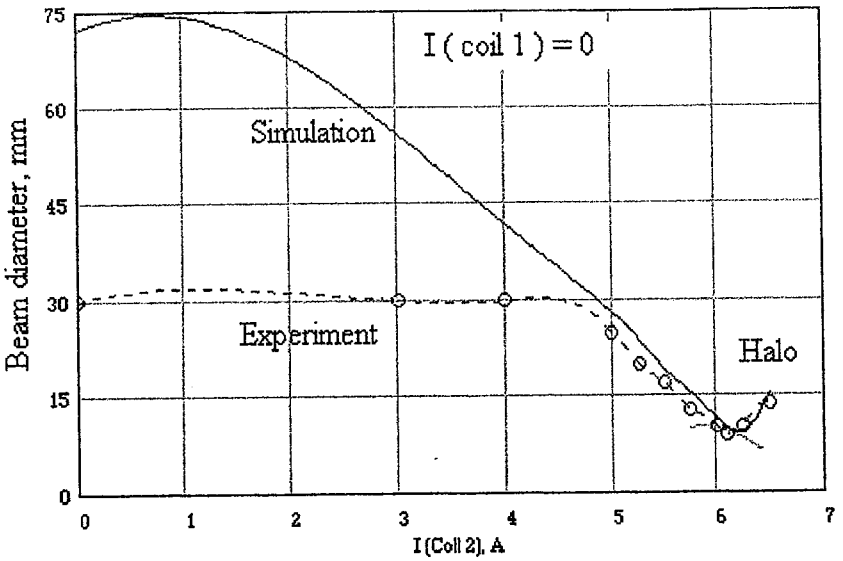

a).

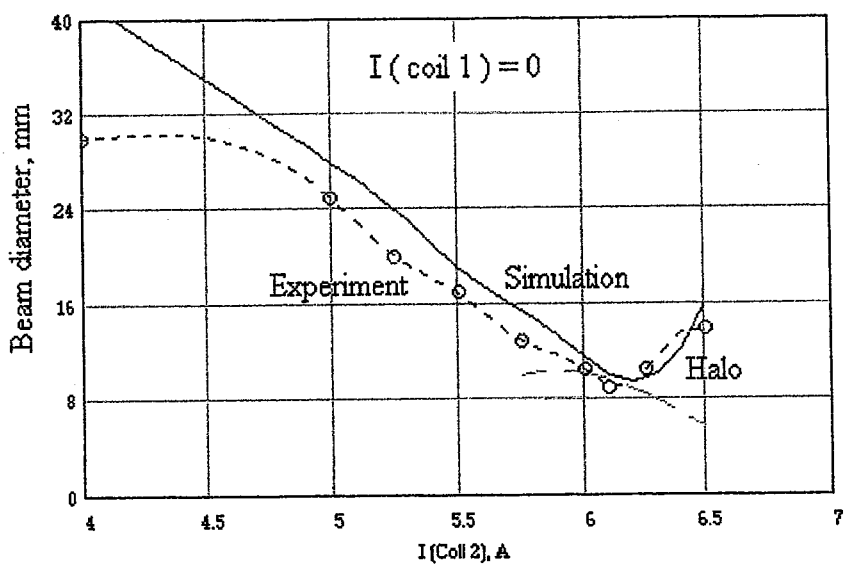

b).

Fig.19a. Simulated and experimental measured beam diameter at the screen position. I (coil1) = 0 and I (coil 2) varied.

Fig.18b. Expansion of the Fig.19a for coil 2 current above 4 Amps.

2. For 43kV cathode-anode voltage.

Simulation parameters: beam current I_{beam}=**1.08A**;
grid – cathode voltage U_{grid}=13kV.

Electron trajectories for the 43kV electron gun is shown in the Fig.20 for I(coil 1) = I(coil 2) = 6A. The radial current density distribution and electrons phase space at the screen are shown in the Fig.21 and Fig.22 respectively. Coil currents are not optimal for the 43kV electron gun. The field is too strong and the maximal beam envelope is larger as compared to the 60kV gun. The beam emittance for 43kV is 127mm*mrad and for 60kV is 60mm*mrad. The normalized beam emittance: ε_N(43kV)=53mm*mrad; ε_N(60kV)=30mm*mrad.

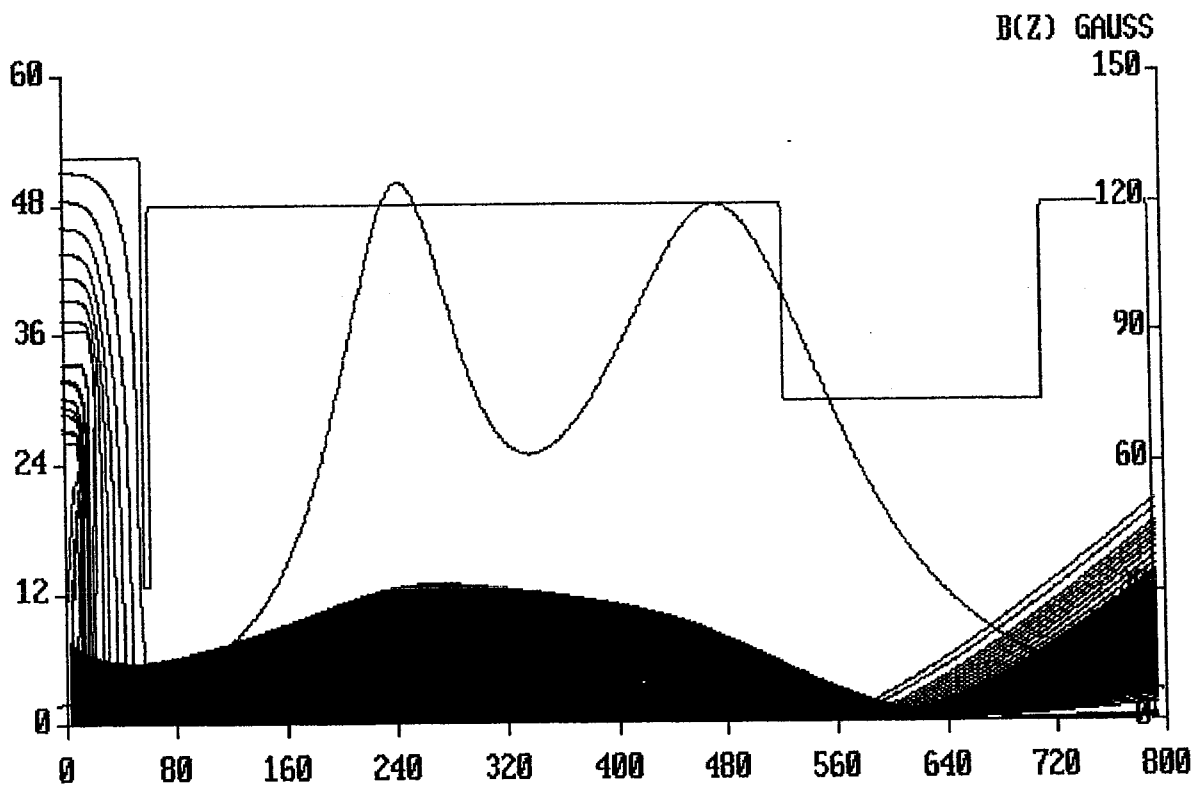

Fig.20. Electron trajectories for **43**kV electron gun. I_{beam}=**1.08A**. Coil currents are: I(coil 1)=I(coil 2) = **6A**.

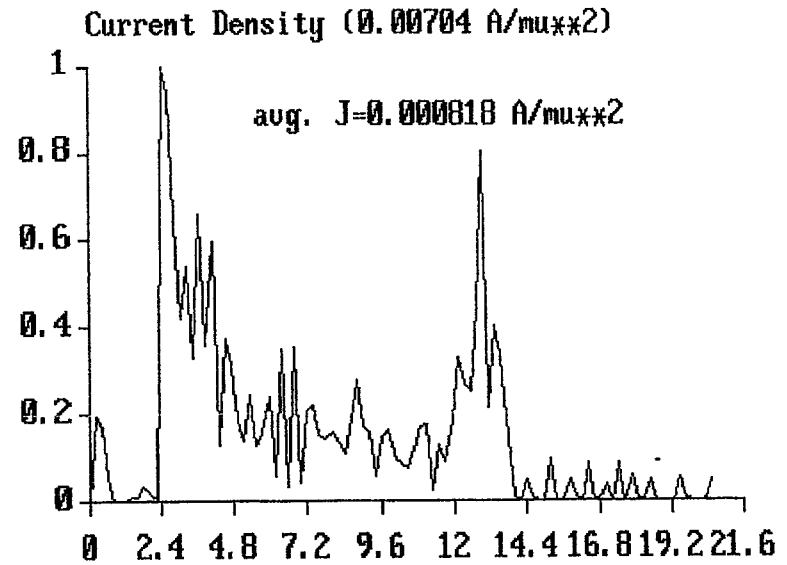

Fig.21. Radial beam density distribution on the screen for U=43kV; I_{beam}=1.08A., I(coil 1)= I(coil 2) = 6A .

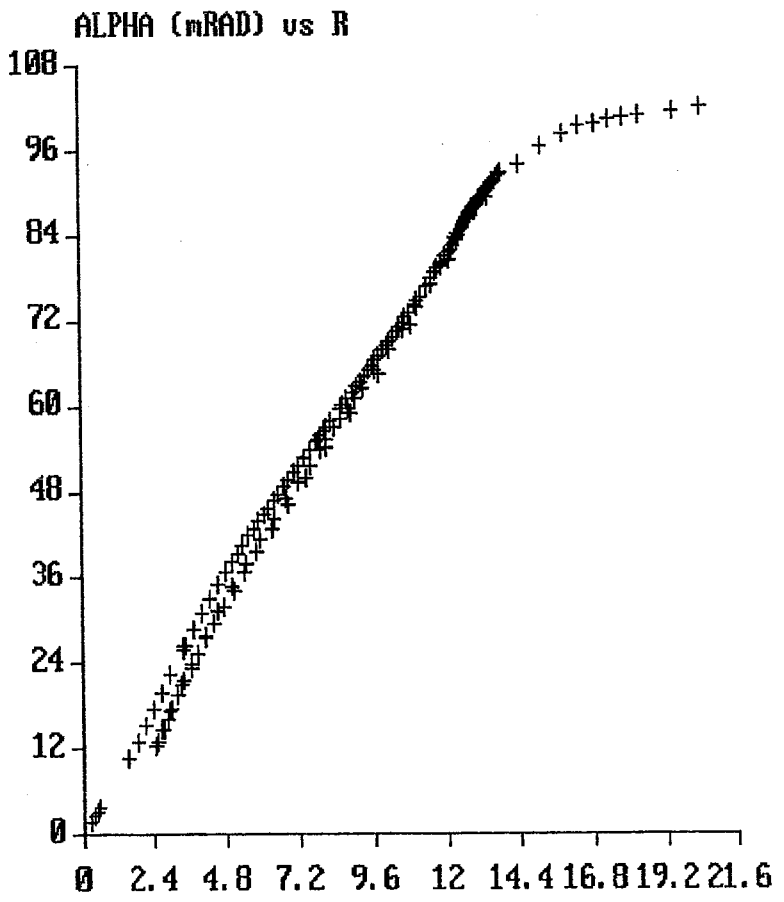

Fig.22. Electrons in the phase space at the screen for U=43kV; I_{beam}=1.08A, I(coil 1) =I(coil 2) = 6A .

Results of simulations and the beam diameters measured at the screen for the 43kV gun are shown in Figs23-30.

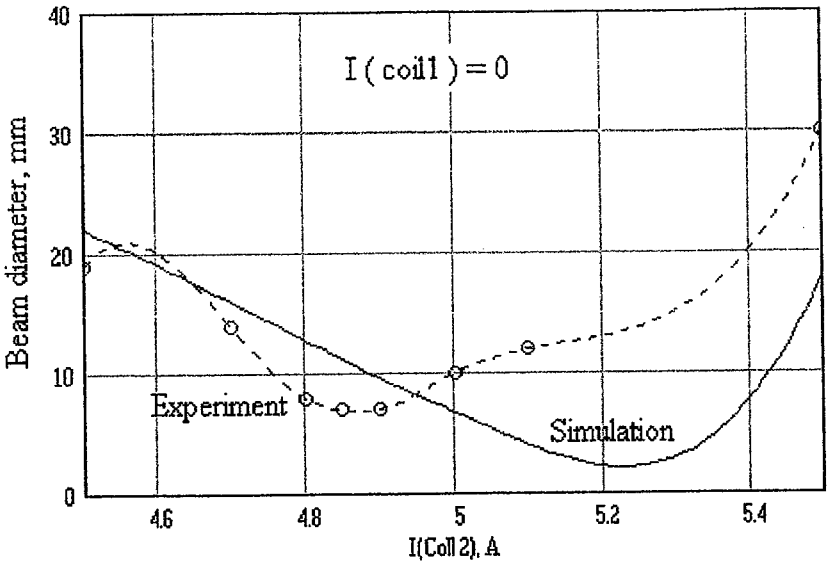

Fig.23. Simulated and experimental measured beam diameter at the screen position for the 43kV gun. I (coil1) = 0 and I (coil 2) varied.

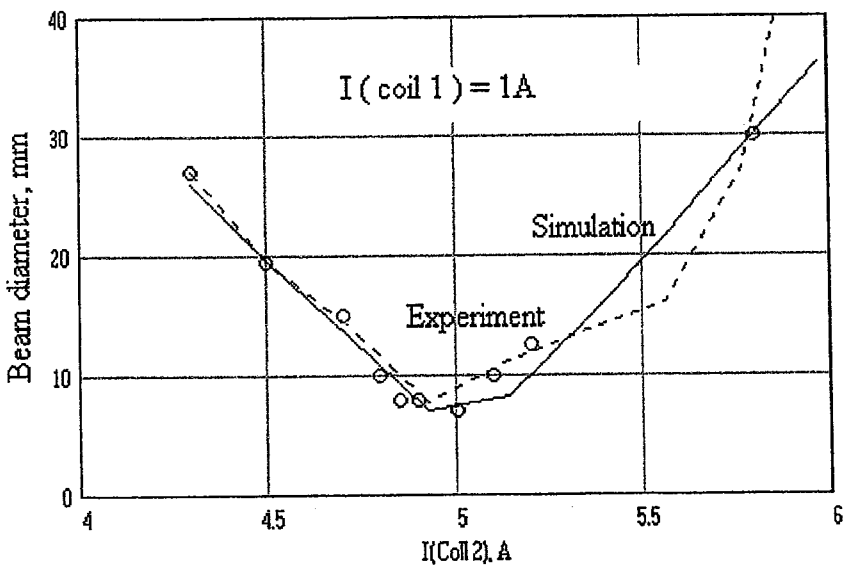

Fig.24. Simulated and experimental measured beam diameter at the screen position for the 43kV gun. I (coil1) = 1A and I (coil 2) varied.

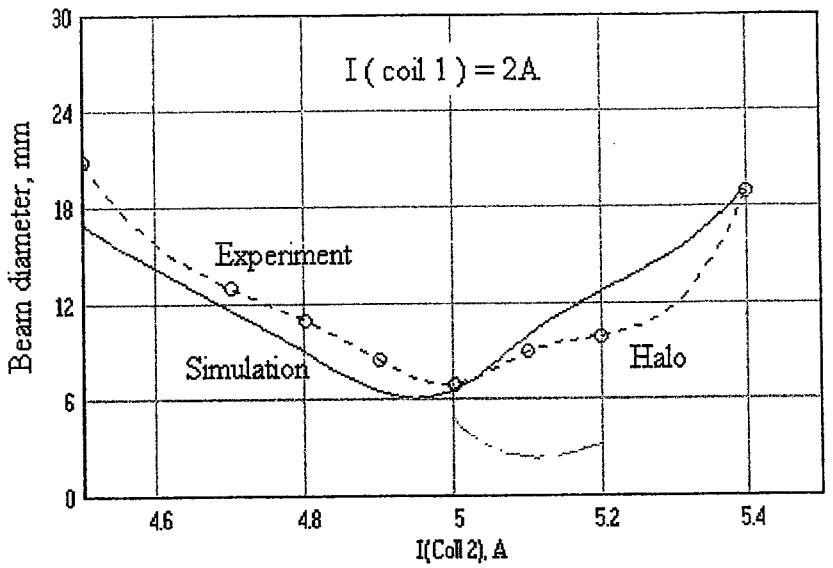

Fig. 25. Simulated and experimental measured beam diameter at the screen position for the 43kV gun. I (coil1) = 2A and I (coil 2) varied.

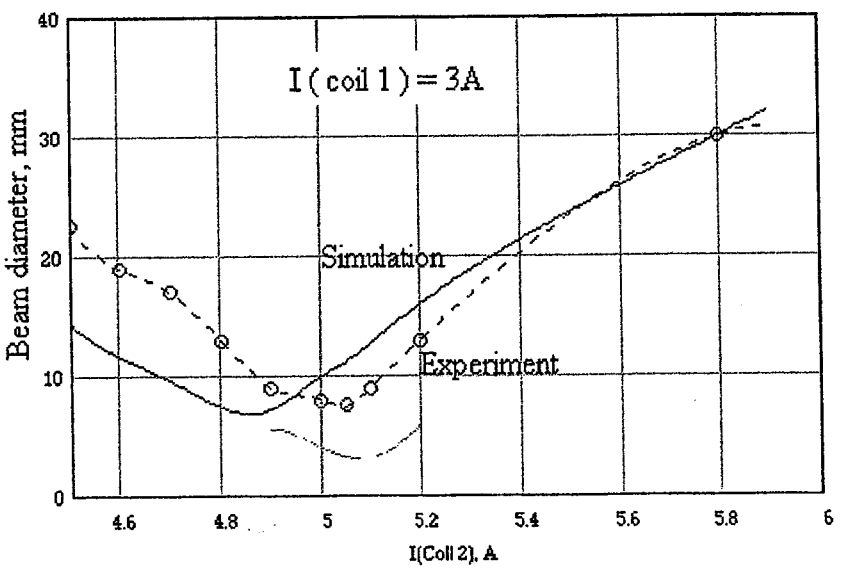

Fig.26. Simulated and experimental measured beam diameter at the screen position for the 43kV gun. I (coil1) = 3A and I (coil 2) varied.

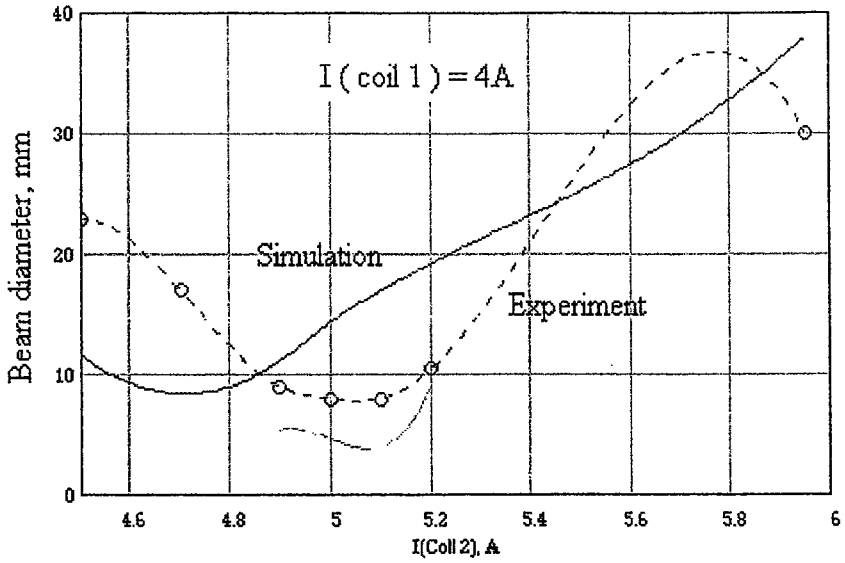

Fig.27. Simulated and experimental measured beam diameter at the screen position for the 43kV gun. I (coil1) = 4A and I (coil 2) varied.

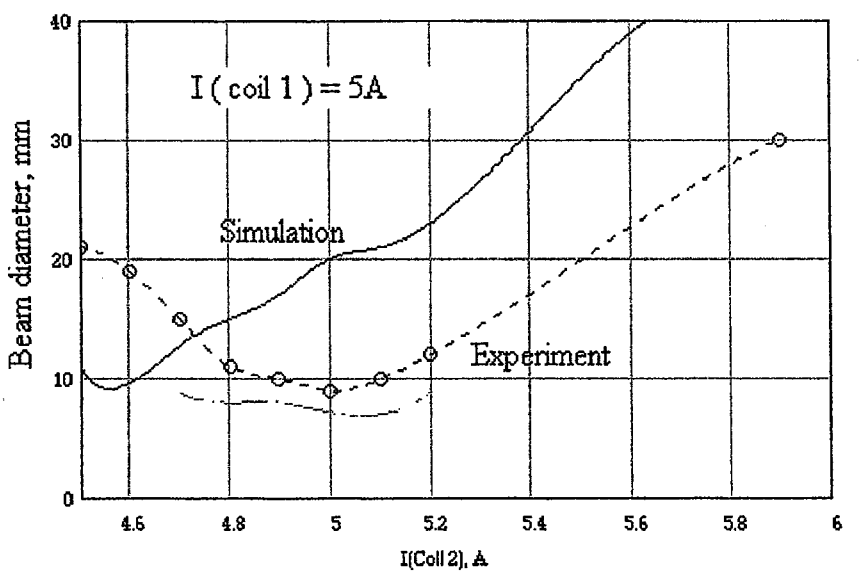

Fig.28. Simulated and experimental measured beam diameter at the screen position for the 43kV gun. I (coil1) = 5A and I (coil 2) varied.

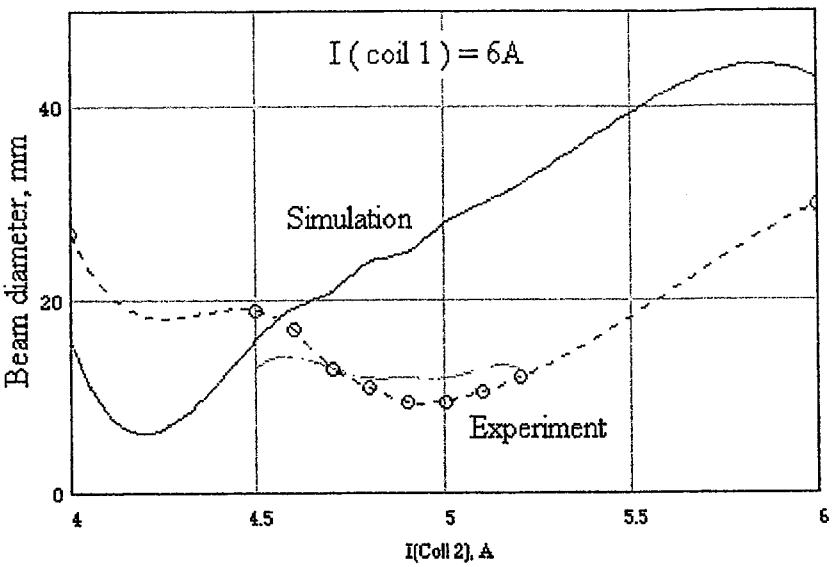

Fig.29. Simulated and experimental measured beam diameter at the screen position for the 43kV gun. I (coil1) = 6A and I (coil 2) varied.

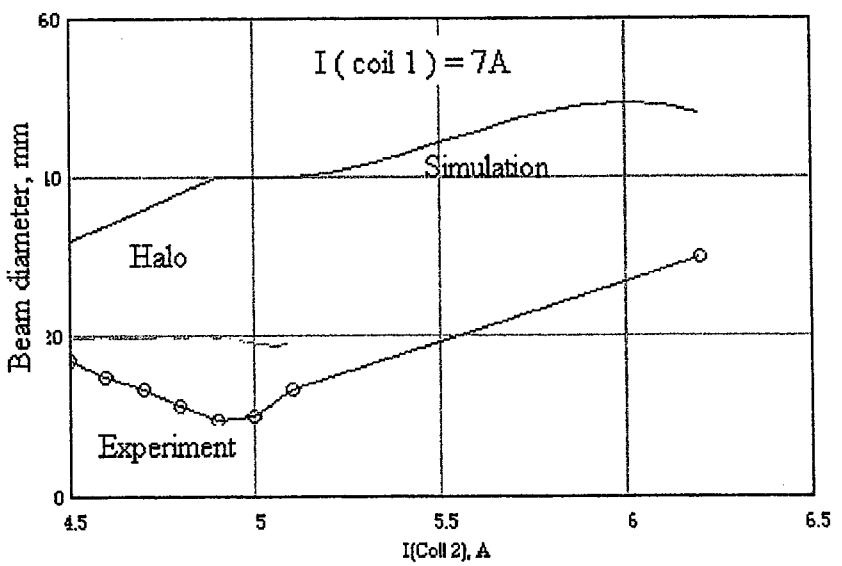

Fig.30. Simulated and experimental measured beam diameter at the screen position for the 43kV gun. I (coil1) = 7A and I (coil 2) varied.

CONCLUSIONS

1. For the 60kV electron gun agreement between measured and simulated results is seen to be fair (see Figs 1-19). For 43kV regime the agreement becomes poorer (see Figs.20-30), particularly for coil2 currents 0A, 4A, 5A, 6A, 7A.
2. The influence of the coil1 current on the beam radius at the target (screen) is relatively small. The ratio of maximum beam envelope radius is only 1.4÷1.5 for a coil1 current change from 0 to 6 Amp.
3. For coil2 current in the range 5.5A÷6Amps a halo due to space charge effects is observed (Figs. 1-3).
4. Optimal currents for focusing coils are as follow: I(coil1)=5÷6Amps, I(coil2)=5.5÷5.7Amps. A change of coil2 current direction influences the electron distribution in the phase space, but does significantly change the beam envelope and the maximum beam divergence.
5. Really optimal currents of the coils together with other 2 focusing short solenoids may be obtained by carrying out a series of beam transport simulations up to the accelerator entrance. For a beam transport system, which includes two addition short focusing solenoids, we can obtain the optimal currents for all the focusing coils.